

1 **A Multi-Criteria Decision Making Approach to the Formulation and**
2 **Selection of Anti-icing Liquids**

3
4 Xianming Shi, Ph.D., P.E.*
5 Western Transportation Institute
6 Associate Research Professor, Civil Engineering
7 Montana State University
8 PO Box 174250
9 Bozeman, MT 59717-4250
10 Phone: (406) 994-6486
11 Fax: (406) 994-1697
12 Email: xianming_s@coe.montana.edu

13
14 Michelle Akin, M.Sc.
15 Research Associate
16 Western Transportation Institute
17 Montana State University
18 PO Box 174250
19 Bozeman, MT 59717-4250
20 Phone: (406) 994-6356
21 Fax: (406) 994-1697
22 Email: michelle.akin@coe.montana.edu

23
24 *Corresponding author

25
26
27 Prepared for the 90th Annual Meeting of the Transportation Research Board
28 Washington, DC
29 January 23–27, 2011

30
31 TRB Committee: Winter Maintenance

32
33 Word Count: 4742; 3 Tables, 7 Figures = 2500 words

34
35
36 Submission Date: July 30, 2010

37
38 **Revision Date: Nov. 15, 2010**

39 **ABSTRACT**

40

41 To effectively fight snow storms in the challenging funding environment, many maintenance
42 agencies in North America have started to produce their own anti-icing liquids, instead of
43 procuring commercial anti-icers. This work demonstrates a systematic approach to data-driven,
44 multi-criteria decision-making, by conducting a set of laboratory tests to assess twenty blended
45 chloride-based anti-icing formulations. The laboratory data were then used to establish predictive
46 models correlating the multiple design parameters with the anti-icer performance and impacts or
47 with an *anti-icer composite index*. We used artificial neural networks for modeling and examined
48 anti-icer performance (characteristic temperature and ice-melting capacity at 30°F and 15°F
49 respectively) and impacts (splitting tensile strength of concrete after ten freeze-thaw cycles and
50 corrosivity to mild steel) as a function of the formulation design. The *anti-icer composite index*
51 was calculated for four different user priority scenarios (*cost-first*, *performance-first*, *impacts-*
52 *first*, or a *balanced approach*), each of which placed a different set of decision weights on
53 various target attributes. Three-dimensional response surfaces were then constructed to illustrate
54 such predicted correlations and to guide the direction for formulation improvements.

55 BACKGROUND

56

57 In the last decades, maintenance agencies in North America have increasingly relied on the use
58 of chemicals to provide reasonably safe driving conditions on the winter road surface. Currently,
59 the United States applies approximately 20 million tons of salts each year for winter road
60 maintenance. This is partially owing to the negative impact of abrasives on water quality and
61 aquatic species, air quality, vegetation, and soil and the hidden cost of sanding [1,2]. It has been
62 recognized that the detrimental environmental impacts of abrasives are generally greater than
63 those of chemicals [3]. The increased use of chemical deicers and anti-icers has also raised
64 concerns about their effects on motor vehicles, the transportation infrastructure, and the
65 environment [4, 5, 6].

66 More recent years have seen the transition from mostly deicing to anti-icing wherever
67 possible [7], in light of the multiple benefits of the latter (e.g., improved level of service, reduced
68 need for chemicals, and associated cost savings and safety/mobility benefits) [8,9]. In current
69 practice, liquid chemicals are used either for anti-icing or in conjunction with applications of
70 solid chemicals and abrasives (i.e., pre-wetting). It is desirable to further expand the use of liquid
71 chemicals such that the overall use of abrasives and solid chemicals can be significantly reduced
72 while maintaining or enhancing the level of service on winter roads.

73 Chloride-based salts are the most common chemicals used to serve as freezing-point
74 depressants for winter road maintenance applications. Sodium chloride (NaCl) is the most
75 widely used chemical due to its abundance and low cost. Magnesium chloride ($MgCl_2$) brines
76 are often used instead of NaCl, and laboratory tests have demonstrated that they exhibit better
77 ice-melting performance at lower temperatures [10]. Field studies have shown calcium chloride
78 ($CaCl_2$) to be more effective than NaCl, owing to its ability to attract moisture and stay on the
79 roads [11]. However, some agencies choose not to use $CaCl_2$ as it does not dry and can cause
80 roads to become slippery [12]. Chlorides are generally considered the most corrosive winter
81 maintenance chemicals [13]; commercially available, corrosion-inhibited versions of these
82 chemicals are often used to reduce their corrosive effects on metals. In addition, acetates and
83 formates are available for anti-icing applications but are much more costly and thus rarely used
84 by highway agencies. Also available are a variety of chemicals derived from agricultural
85 byproducts, used either alone or as additives for deicers or anti-icers.

86 To effectively fight snow storms in the challenging funding environment, many
87 maintenance agencies in North America have started to produce their own anti-icing liquids,
88 instead of procuring commercial anti-icers. Such “brine-making” operations not only can result
89 in cost savings and enhance the agency preparedness during winter storms, but also allow
90 agencies to blend different liquid chemicals for improved performance at lower temperatures.
91 While a variety of laboratory tests exist for assessing deicers or anti-icers, research is still needed
92 to improve the knowledge of performance characteristics of blended liquid products and their
93 deleterious impacts on motor vehicles and transportation infrastructure. Research is also needed
94 to establish a framework that would enable data-driven decision-making when it comes to
95 selecting or formulating anti-icing liquids for snow and ice control. This can be accomplished by
96 integrating agency priorities with laboratory testing data wherever possible. As such, each
97 agency can take a holistic approach to anti-icer procurement or design, and strike the right
98 balance in meeting its multiple goals of winter maintenance, including safety, mobility,
99 environmental stewardship, infrastructure preservation, and economics.

100 This work demonstrates a systematic approach to data-driven, multi-criteria decision-
101 making, by conducting a set of laboratory tests to assess twenty blended chloride-based anti-
102 icing formulations. The laboratory data were then used to establish predictive models correlating
103 the multiple design parameters with the anti-icer performance and impacts or with an anti-icer
104 composite index and to construct response surfaces illustrating such correlations.

105

106 **METHODOLOGY**

107

108 **Design of Experiments**

109 When blending various amounts of corrosion inhibitor, MgCl_2 and CaCl_2 into the NaCl brine,
110 the resultant anti-icer is expected to change its performance and impacts. In this study, we used a
111 unique tool for the statistical design of experiments, known as *uniform design* [14], to reduce the
112 number of experiments needed to explore a large unknown domain of anti-icer design parameters
113 and to capture their complex interactions. We chose to investigate only twenty anti-icer
114 formulations by adopting the design parameters and associated target attributes as shown in
115 Table 1. Note that there would be a total of $4 \times 4 \times 5 = 80$ formulations to be investigated in the
116 absence of a statistical design, as the dosage of MgCl_2 , CaCl_2 , and corrosion inhibitor (GLT)
117 varied at 4, 4, and 5 levels respectively.

118
119

TABLE 1 Experimental data used for ANNs training and testing (with asterisk) respectively

Anti-icer Mix No.	MgCl ₂ ·6H ₂ O (g/g NaCl)	CaCl ₂ ·2H ₂ O (g/g NaCl)	GLT (mL/g NaCl)	T_c (°F)	IMC, 15°F, 60 min (%) mL/mL	IMC, 30°F, 60 min (%) mL/mL	Predicted PCR	Freeze- Thaw Mass Loss (%)	STS after Freeze- Thaw (psi)	Thaw Mass Loss Index	Freeze Thaw STS Index	Estimated Cost (dollars/ gallon)	Composite Index 1	Composite Index 2	Composite Index 3	Composite Index 4
1	0.968	0.326	0.129	24.52	133.2	388.9	14.5	2.69	1014.51	46.2	31.4	0.27	73.6	84.9	38.3	65.0
2	0.646	1.305	0.194	22.11	129.5	414.9	15.9	5.97	569.71	110.8	133.2	0.39	28.0	46.8	58.1	46.5
3	0.968	1.304	0.258	19.47	128.4	441.2	16.2	3.83	577.76	68.8	131.3	0.42	21.8	58.9	87.2	61.4
4	0.323	0.978	0.129	24.15	135.6	390.6	17.8	5.06	647.84	93.0	115.3	0.31	53.4	52.7	38.3	46.9
5	0.646	0.652	0.258	24.35	91.8	421.2	13.1	4.01	741.86	72.3	93.8	0.32	53.1	65.6	36.4	51.6
6	0.646	0.652	0.065	24.52	123.2	396.2	12.5	1.96	883.30	31.8	61.5	0.28	70.4	83.2	37.8	63.4
7	0.646	0.652	0	24.25	143.6	383.7	61.9	4.83	684.38	88.5	107.0	0.26	65.4	20.6	35.0	35.5
8	0.323	0.326	0.129	25.44	72.1	425.2	10.3	2.76	829.62	47.7	73.7	0.22	86.0	78.8	27.4	60.6
9	0.646	0.978	0.065	23.08	137.8	399.3	18.9	6.37	649.04	118.7	115.0	0.32	51.4	46.8	49.1	48.0
10	1.291	0.652	0.194	22.37	131.9	410.5	11.6	2.19	826.66	36.5	74.4	0.34	48.7	81.0	59.6	66.2
11	0.323	0.652	0.194	24.85	134.0	385.0	13.2	1.66	956.51	26.0	44.7	0.28	68.3	87.1	34.6	63.5
12	0.968	0.978	0.129	22.14	131.0	413.4	11.1	2.36	877.14	39.7	62.9	0.35	46.5	83.2	62.1	67.6
13	0.646	0.652	0	23.94	129.9	396.9	57.2	2.23	835.65	37.2	72.4	0.26	69.8	44.1	40.5	48.6
14	0.646	0.326	0.258	25.08	126.9	388.2	13.2	2.64	871.30	45.3	64.2	0.27	69.4	78.3	31.3	58.7
15	1.291	0.326	0	23.78	133.5	395.7	63.5	3.66	758.44	65.4	90.0	0.26	67.8	28.8	40.8	41.8
16	1.291	1.304	0.065	19.81	144.5	425.9	16.4	4.50	747.12	81.9	92.6	0.40	29.2	64.0	84.7	64.2
17	0.646	0.978	0.194	23.12	131.9	403.3	13.1	1.72	875.86	27.0	63.2	0.34	47.7	83.6	51.7	64.2
18*	0.323	1.304	0	23.06	137.4	399.8	13.1	3.37	702.91	59.7	102.7	0.33	52.0	68.0	51.3	58.0
19	0.968	0.652	0.065	23.32	130.1	402.6	12.4	2.69	740.20	46.2	94.2	0.30	63.3	73.9	49.5	62.2
20	1.291	0.652	0.258	22.23	142.1	404.3	12.6	2.82	800.68	48.9	80.4	0.36	43.3	75.9	60.5	63.2

120
121
122
123
124
125

Note: 1. Only the target attributes highlighted with bold fonts were quantitatively modeled using neural networks. 2. T_c = characteristic temperature derived from Differential Scanning Calorimetry (DSC) thermograms; *IMC* = ice-melting capacity; *PCR* = Percent Corrosion Rate; *STS* = Splitting Tensile Strength. 3. The composite indices were calculated for four different user priority scenarios respectively, i.e., *cost-first*, *performance-first*, *impacts-first*, or a *balanced approach*.

126 Anti-icing Formulations and Laboratory Tests

127 Understanding the performance characteristics and negative impacts of anti-icers is
 128 critical to effective and responsible winter maintenance operations. As such, laboratory
 129 tests were conducted to assess the performance of blended chloride brines and their
 130 impacts on metal, concrete and asphalt. To prepare the anti-icer formulations shown in
 131 Table 1, we used reagent-grade chloride chemicals and de-ionized water, whereas in
 132 practice maintenance agencies would have used less pure chemicals and tap water. A
 133 commercial corrosion inhibitor, GLT from Paradigm Chemical (Acworth, Georgia) was
 134 used in some blends. Each formulation had the same amount of NaCl (116 grams per
 135 Liter) and various amounts of CaCl_2 , MgCl_2 , and GLT (which were determined using the
 136 uniform design table).

137 The performance characteristics of anti-icers were assessed by measuring their
 138 Differential Scanning Calorimetry (DSC) thermogram with a TA Instruments Q200
 139 apparatus. The use of DSC to quantify deicer or anti-icer performance is relatively new [15],
 140 even though it has been widely employed to rapidly and consistently characterize and
 141 quantify the thermal properties of materials. The thermograms were measured in the
 142 temperature range of 25 to -60°C (77 to -76°F) with a cooling/heating rate of 2°C (3.6°F)
 143 per minute. The anti-icers were first diluted using the anti-icer/water volume ratio of
 144 1.5:1 and then allowed to reach ambient temperature. Subsequently, ten μL samples were
 145 pipetted into an aluminum sample pan and hermetically sealed for DSC measurements. At
 146 least three samples were run for each anti-icer to minimize data variability. The first peak
 147 at the warmer end of the heating cycle thermogram was used to derive the characteristic
 148 temperature of the anti-icer tested (T_c), which along with the heat flow (H , integrated
 149 surface area of the peak) are used to estimate the ice melting capacity (IMC) of the anti-
 150 icer at 60 minutes of application. Specifically, the IMC of anti-icers at 60 minutes were
 151 estimated for 15°F and 30°F respectively, using the following equations [15]:

$$152 \quad IMC_{30^\circ\text{F}} \left(\%, \frac{\text{mL melt}}{\text{mL applied}} \right) = [-0.02265T_c + 1.965 \log(\Delta H) + 0.03285t - 2.1761] / 0.9 \cdot 100 \quad (1)$$

$$153 \quad (R^2 = 0.94)$$

$$154 \quad IMC_{15^\circ\text{F}} \left(\%, \frac{\text{mL melt}}{\text{mL applied}} \right) = [-0.08667T_c - 2.6511 \log(\Delta H) - 0.000716t + 9.114] / 0.9 \cdot 100 \quad (2)$$

$$155 \quad (R^2 = 0.80)$$

Where:

IMC = Amount of ice melted per unit of brine applied (%)

ΔH = 345 J/g minus heat flow (H in J/g) of characteristic peak from DSC (J/g)

T_c = characteristic temperature from DSC ($^\circ\text{F}$)

t = time between 10 and 60 (minutes)

152
 153 The corrosion of anti-icers to mild steel (ASTM A36) was assessed using a three-
 154 electrode electrochemical cell and a Gamry Instruments[®] Potentiostat with an 8-channel
 155 Electrochemical Multiplexer. Each anti-icer formulation prepared was further diluted by
 156 water at 3:100. Prior to testing, the steel coupons were cleaned with acetone and de-
 157 ionized water. For each anti-icer, four steel coupons were subjected to wet-dry cycling in
 158 the diluted anti-icer as follows: 1-hour wet, 4-hour dry, 1-hour wet, 16-hour dry, 2-hour

159 wet. For each steel coupon, a weak polarization curve was measured at the end of the 24-
 160 hour cycle, from which its corrosion potential (E_{corr}) was derived. As such, the
 161 electrochemical technique provides an alternative to the gravimetric method in rapidly
 162 assessing corrosivity of solutions. The corrosivity of each anti-icer was reported as
 163 Percent Corrosion Rate (PCR), as defined in the PNS/NACE corrosion test method,
 164 where it is normalized from actual mass loss of metallic coupons by setting the PCR of
 165 water at 0 and the PCR of a 3% dilution of a 23% NaCl brine solution at 100. In this
 166 study, the PCR values of the anti-icers were estimated from the E_{corr} data, using the
 167 following equation [16]:

$$PCR(\%) = 667.24E_{corr}^2 + 448.93E_{corr} + 83.184 \quad (3)$$

Where E_{corr} = Corrosion potential (mV, vs. Ag/AgCl)

168
 169 The impacts of anti-icers on concrete were assessed by conducting freeze-thaw
 170 tests of Portland cement concrete (PCC) samples in the presence of anti-icers, following
 171 the SHRP H205.8 test method with minor modifications. The test evaluates the combined
 172 effects of liquid chemicals and freeze-thaw cycling on the structural integrity of
 173 specimens of non-air-entrained concrete. Concrete samples were made in 1½" diameter ×
 174 1⅞" length (3.8 cm × 4.8 cm) poly(vinyl chloride) piping with a volume of 54 cm³. The
 175 concrete mix design had a water-to-cement ratio of 0.55, a slump of 5.5" (14 cm) and air
 176 content of 1.6 percent. Samples were cured in water in the first 24 hours before being
 177 placed in a container with 100 percent relative humidity. The average 28-day
 178 compressive strength of three test cylinders was 7474 psi (51.5 MPa). The dry weight of
 179 each sample was recorded before placing it on a sponge inside a dish containing 310 mL
 180 of diluted (3%) anti-icer solution. The dish was covered in plastic wrap to press the
 181 concrete samples into the sponge and then placed in a Ziploc bag. Three concrete
 182 specimens were tested in each anti-icer solution. There were two controls: 1) a 3% NaCl
 183 solution and 2) de-ionized water. A thermocouple was embedded in one of the control
 184 concrete samples to monitor temperatures during freeze-thaw cycling. The sealed dishes
 185 were placed in the freezer for 16 to 18 hours at $-17.8 \pm 2.7^\circ\text{C}$ ($0 \pm 4.9^\circ\text{F}$), then placed in
 186 the laboratory environment at $23.0 \pm 1.7^\circ\text{C}$ ($73.4 \pm 3^\circ\text{F}$) for 6 to 8 hours. This cycle was
 187 repeated for 10 days. The test specimens were then removed from the dish and rinsed
 188 under running water to remove any scaled-off material. The specimens were air-dried
 189 overnight before the final weight of each was recorded.

190 The mass loss due to freeze-thaw exposure was relatively minor for most concrete
 191 specimens. Therefore, the concrete specimens were also tested for splitting tensile
 192 strength. The specimens were laid on their side with a thin wooden stick above and below
 193 where the specimen contacted the compressive testing machine. Compressive stress
 194 caused the specimens to split in half; the maximum load was used to calculate the
 195 splitting tensile strength (STS) as follows:

$$STS \text{ (psi)} = \frac{P \cdot C}{\pi \cdot L \cdot D} \quad (4)$$

Where:

P = Load at failure (lb)

C = Estimated length of contact on the top and bottom (for undamaged specimens,

$C = 2$; but scaled specimens had lower contact areas, from 0.7 to 1.9)

L = Length of specimen (1.875 in.)

D = Diameter of specimen (1.5 in.)

196

197

198

199

200

201

202

203

204

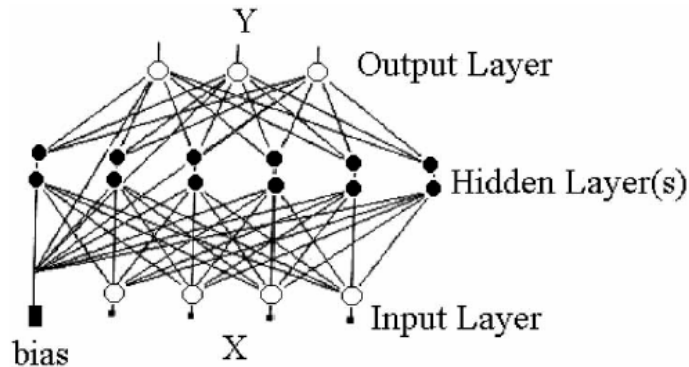
205

206

207

The impacts of anti-icers on asphalt were assessed with a bending beam rheometer (BBR). A PG 64-28 asphalt binder was first aged in a rolling thin film oven to simulate the effects of hot-mixing asphalt concrete. Asphalt binder (in contact with anti-icer solution) was then placed in a pressure aging vessel to simulate 7-10 years of in-service aging. After degassing, beams were molded and tested in the BBR.

The anti-icer mix design and laboratory test results are shown in Table 1. The costs of anti-icer formulations were estimated by assuming the raw material of NaCl, $MgCl_2 \cdot 6H_2O$, $CaCl_2 \cdot 2H_2O$, corrosion inhibitor GLT, and water delivered at \$60, \$150, \$300, \$400 and \$2 per tonne respectively and a mixing cost of \$0.10 per gallon, based on individual communications with winter maintenance practitioners in the United States. These numbers are for demonstration purpose only and may not reflect actual costs.



208

209

210

211

FIGURE 1 A typical multi-layer feed-forward ANN architecture.

212

Modeling Technique

213

214

215

216

217

218

219

220

221

222

223

224

225

226

227

228

229

230

To explore the complex relations between anti-icer design parameters and the resultant performance and impact attributes, artificial neural networks (ANNs) were chosen to be the modeling tool. ANNs provide a non-parametric, self-adaptive approach to information processing and are powerful in tackling complex, non-linear problems [17, 18, 19] where conventional modeling techniques (e.g., multiple regression) fail. We adopted multi-layer feed-forward ANNs for modeling, of which a typical architecture is shown in Figure 1. The nodes in the input and output layers consist of independent variables and response variable(s), respectively, whereas the topological structure of the hidden layer(s) depends on the complexity of the relationships. In this study, a modified back propagation algorithm was employed for the ANN training. The detailed description of data normalization, transfer function, and error propagation algorithm is provided elsewhere [17].

RESULTS AND DISCUSSION

Modeling Technique

The parameters and performance of the ANN models in this study are provided in Table 2. The relatively small training and testing errors show that the established ANN models

231 have good “memory” and the trained matrices of interconnected weights and bias
 232 (“fabric” of the neural networks) reflect the hidden functional relationships well.

233 On a different note, the effort of using ANN to establish a predictive model for
 234 the mass loss of concrete after freeze-thaw exposure led to unreasonable and extremely
 235 irregular predictions. As such, the ANN model was discarded. This failed effort was
 236 consistent with the observation that the mass loss data featured high coefficients of
 237 variance, indicative of noise in the experimental data. This confirms the rule that *the*
 238 *predictive quality of any model would not exceed the quality of the data used to construct*
 239 *it.*

240 **TABLE 2 Parameters and performance of the ANN models in this study**
 241

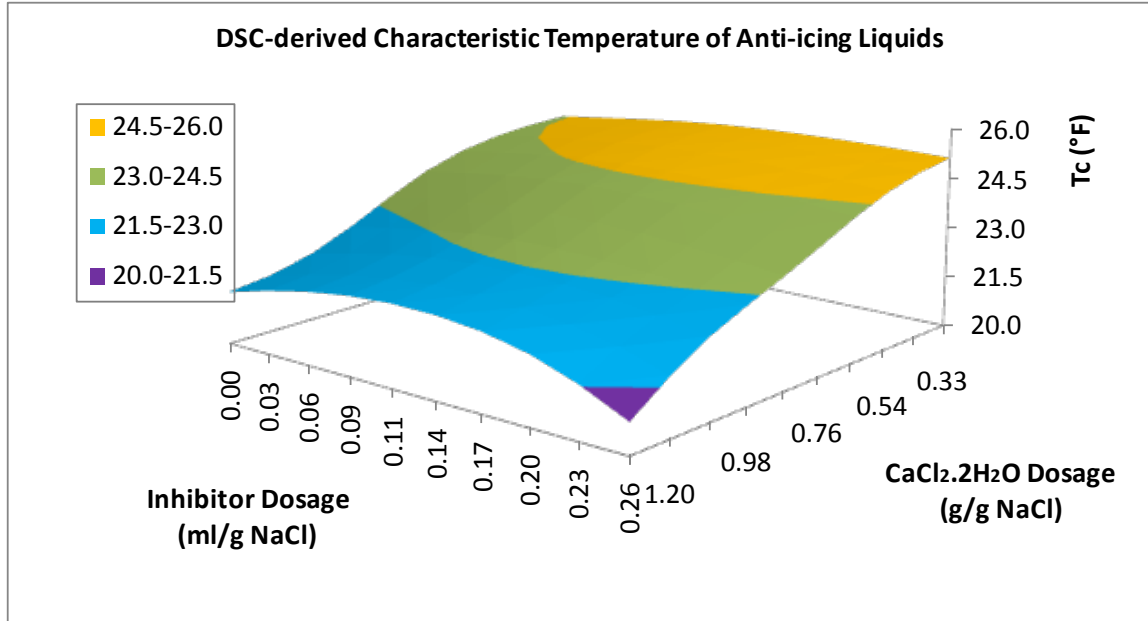
<i>Response Variable</i>	<i>Sum of the Mean Squared Error (SMSE)</i>		<i>Topological Structure of the ANN model</i>
	Training	Testing	
T_c (°F)	0.011	0.012	3-6-1
IMC at 60 min, 15°F (% , mL/mL)	0.038	0.042	3-5-1
IMC at 60 min, 30°F (% , mL/mL)	0.047	0.048	3-5-1
Predicted corrosivity (<i>PCR</i>)	0.021	0.030	3-4-1
STS of concrete after freeze-thaw cycling (psi)	0.049	0.055	3-6-1
Anti-icer composite index 1 (<i>cost-first</i>)	0.012	0.015	3-5-1
Anti-icer composite index 2 (<i>effects-first</i>)	0.057	0.055	3-6-1
Anti-icer composite index 3 (<i>performance-first</i>)	0.015	0.017	3-6-1
Anti-icer composite index 4 (<i>balanced approach</i>)	0.064	0.054	3-6-1

242

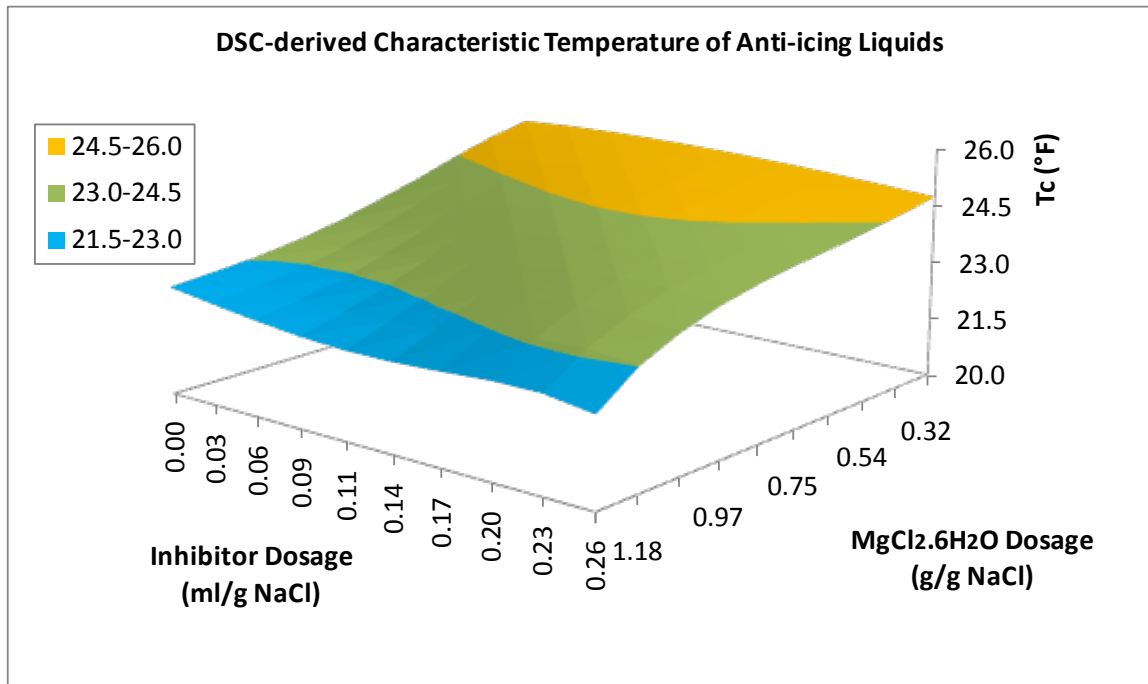
243 **Anti-icer Performance and Impacts**

244 For each anti-icer performance or impact attribute (also termed as “target attribute” or
 245 “response variable”), once the empirical ANN model was trained and tested it was used
 246 to predict the anti-icer property as a function of various design variables. This serves to
 247 identify meaningful trends and to guide the direction for formulation improvements. Such
 248 predictions were made with each design variable varying in the range of training data,
 249 since ANNs are not suitable for extrapolation.

250

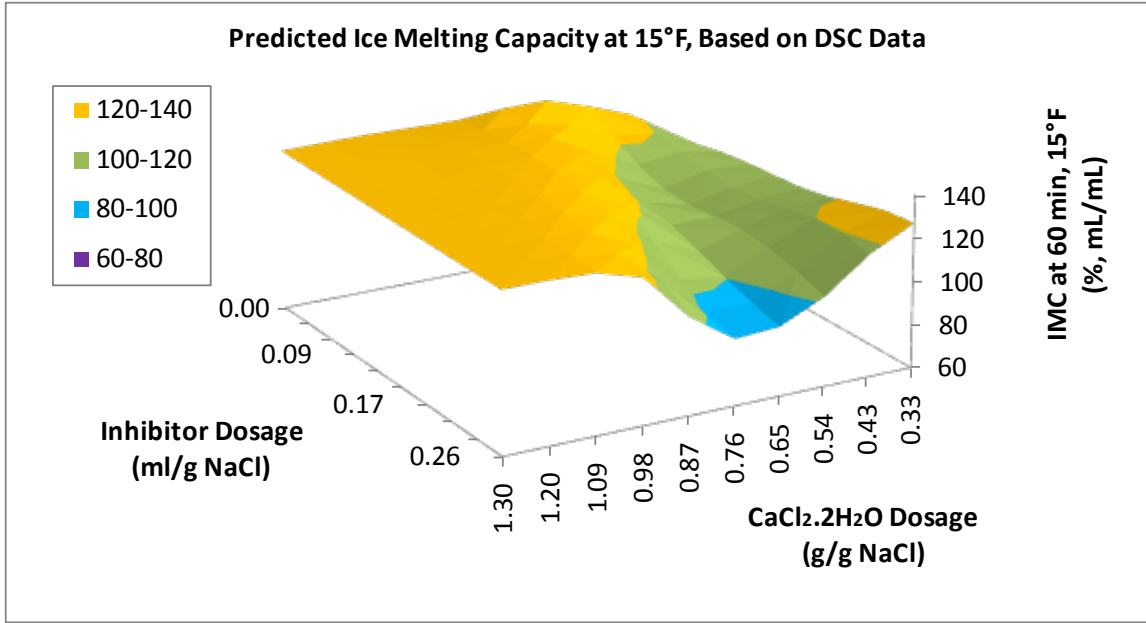


251
252
253



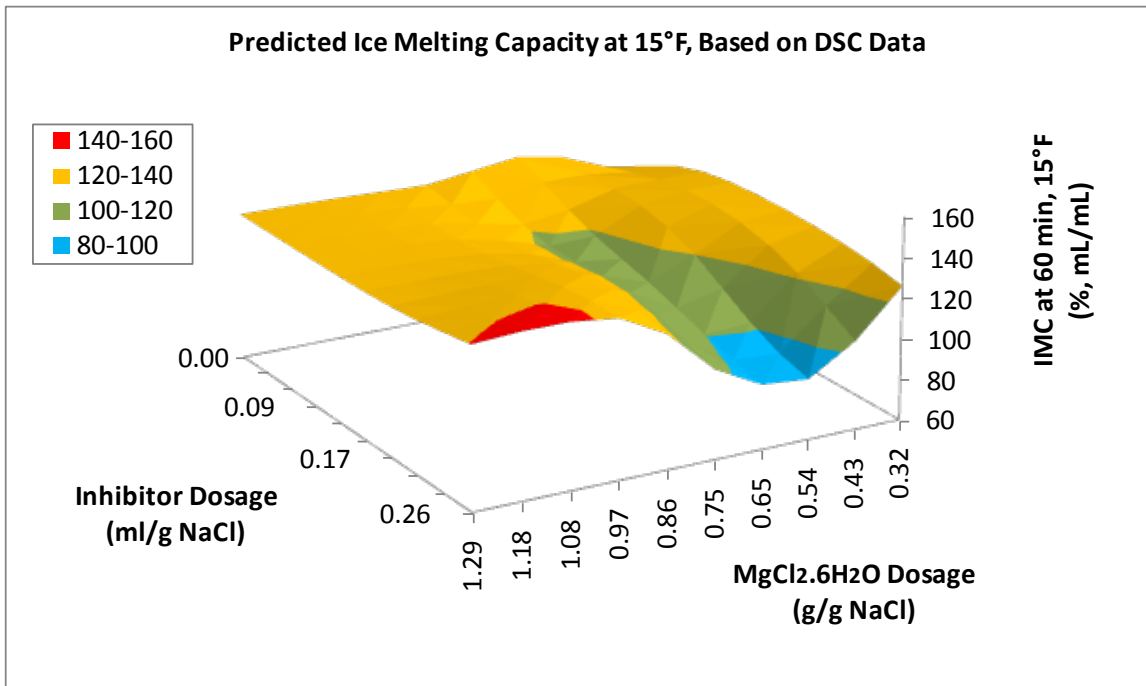
254
255
256
257
258
259

FIGURE 2 Predicted characteristic temperature as a function of (a) inhibitor and calcium chloride dosages, with $\text{MgCl}_2 \cdot 6\text{H}_2\text{O}/\text{NaCl}$ set at 0.65 g/g; (b) inhibitor and magnesium chloride dosages, with $\text{CaCl}_2 \cdot 2\text{H}_2\text{O}/\text{NaCl}$ set at 0.65 g/g.



(a)

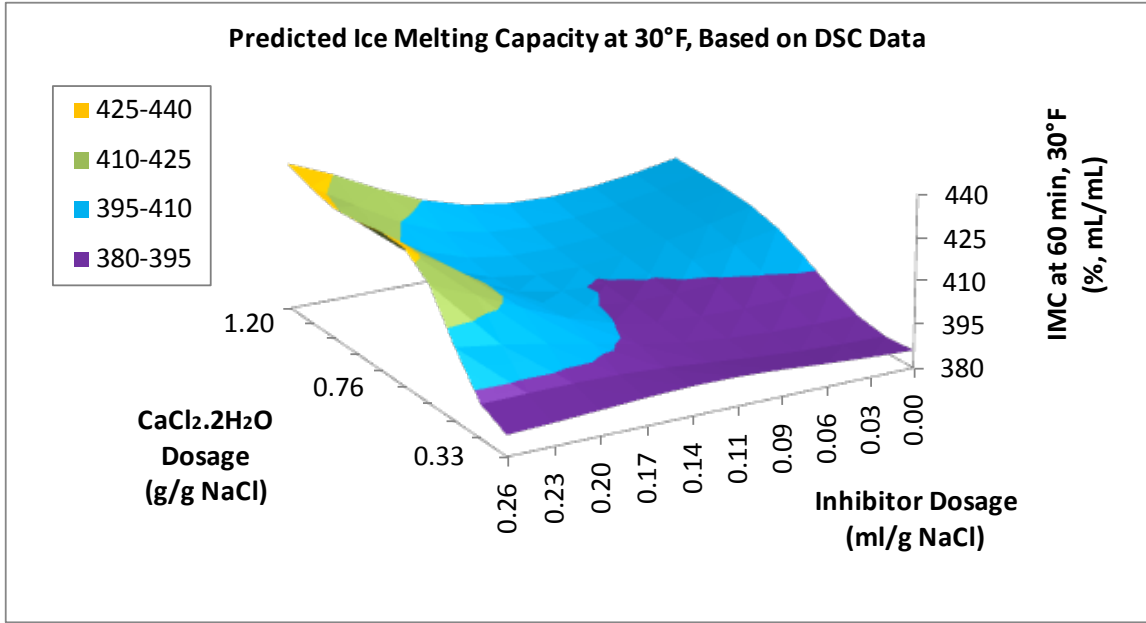
260
261
262



(b)

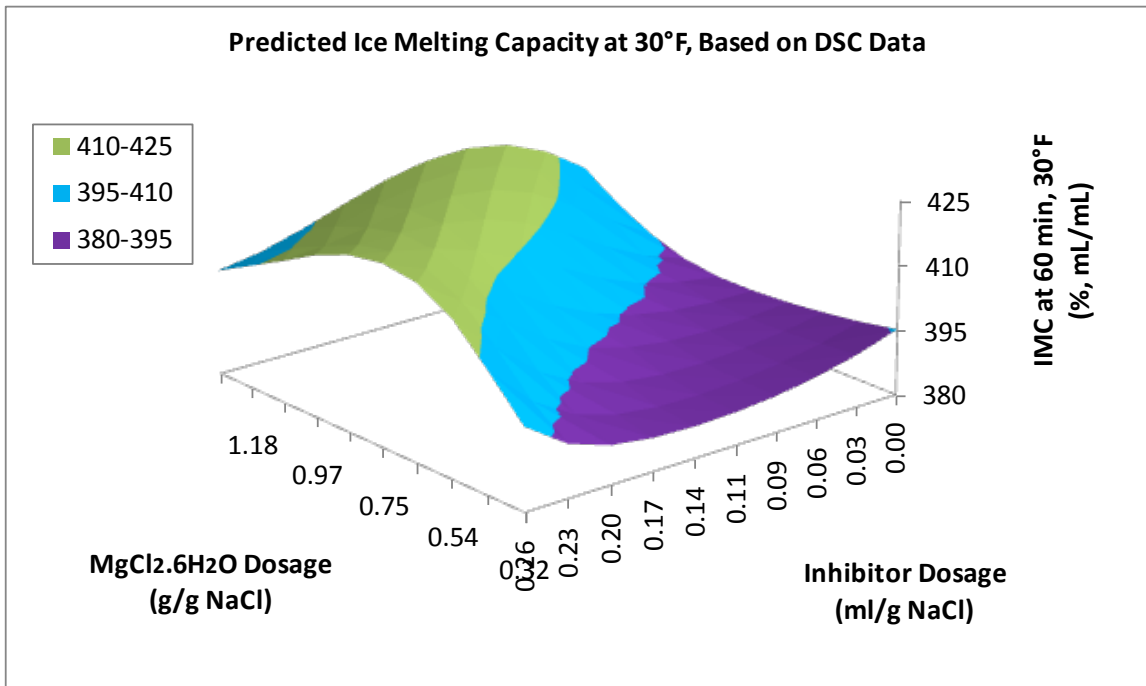
263
264
265
266
267
268
269

FIGURE 3 Predicted ice melting capacity at 60 min, 15°F, as a function of (a) inhibitor and calcium chloride dosages, with MgCl₂·6H₂O/NaCl set at 0.65 g/g; (b) inhibitor and magnesium chloride dosages, with CaCl₂·2H₂O/NaCl set at 0.65 g/g.



(a)

270
271
272



(b)

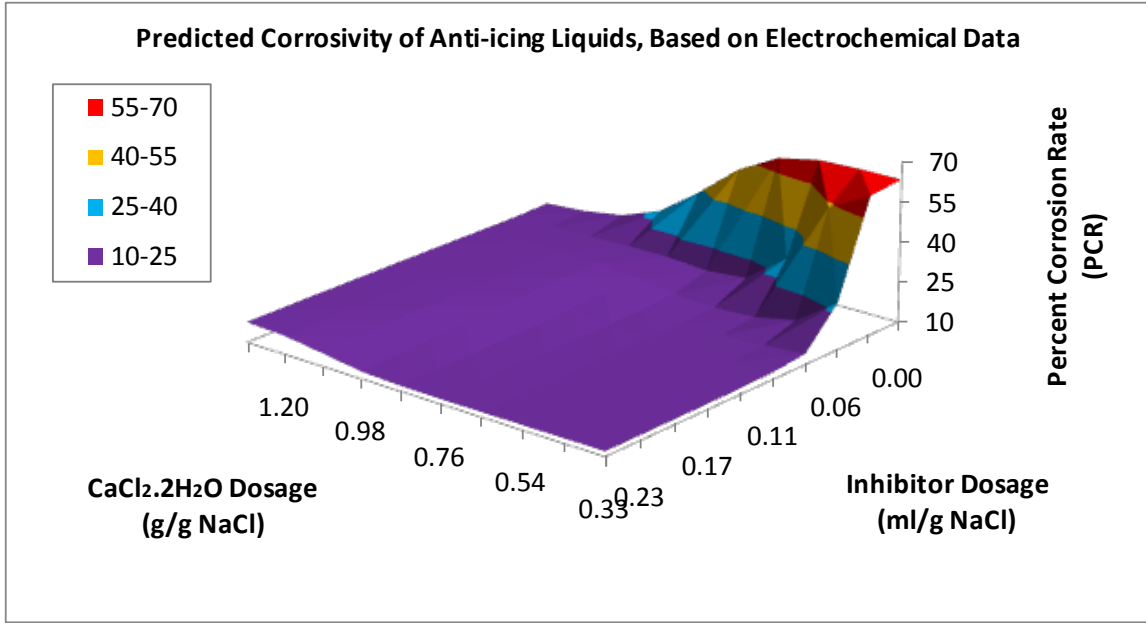
273
274
275
276
277
278
279

FIGURE 4 Predicted ice melting capacity at 60 min, 30°F, as a function of (a) inhibitor and calcium chloride dosages, with $MgCl_2 \cdot 6H_2O/NaCl$ set at 0.65 g/g; (b) inhibitor and magnesium chloride dosages, with $CaCl_2 \cdot 2H_2O/NaCl$ set at 0.65 g/g.

280 The performance characteristics of the anti-icers were assessed using DSC
281 thermograms, which can detect phase transitions and shed light on the thermal behavior
282 of each chloride-water-inhibitor mixture. As shown in Table 1, we used three parameters
283 to characterize the performance of anti-icers: T_c , IMC (60-min) at 15°F (-9.4°C) and at
284 30°F (-1°C), the experimental data of which were used to establish ANN models and to
285 construct response surfaces as shown in Figure 2, Figure 3, and Figure 4 respectively.
286 Figure 2 indicates that T_c tends to decrease as the dosage of calcium chloride or
287 magnesium chloride increases, which suggests the beneficial role of such addition in
288 suppressing the freezing-point temperature of the mixture. It should be noted that the
289 addition of more chlorides into the anti-icer is ultimately limited by the solubility of these
290 chlorides in water. Figure 2 also shows that the effect of inhibitor concentration on T_c is
291 much less obvious.

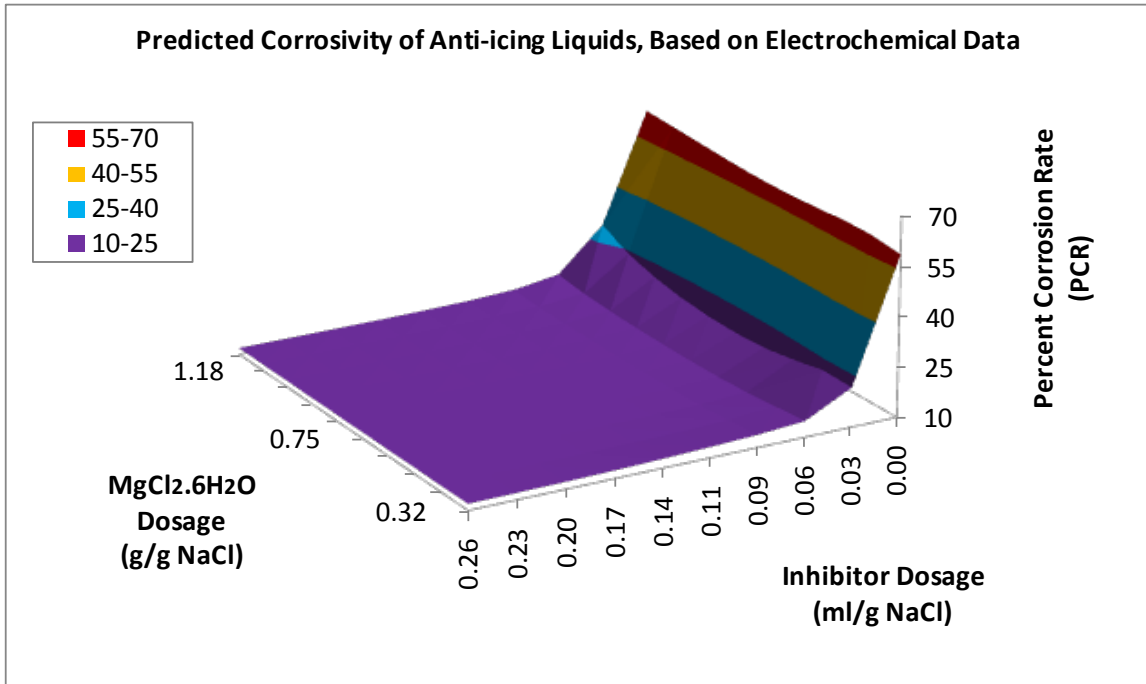
292 Figure 3 and Figure 4 present surface plots that illustrate the highly non-linear
293 nature of the dependency of IMC on the anti-icer mix design, even though the maximum
294 IMC values tend to correspond to high concentrations of calcium chloride or magnesium
295 chloride. Figure 3 shows that the minimum IMC values at 15°F (-9.4°C) correspond to
296 high inhibitor concentrations, when calcium or magnesium chloride by weight of sodium
297 chloride falls in the range of 0.65-0.76. IMC values lower than 100 (% , mL/mL) suggest
298 a negative melting amount, or freezing of the applied anti-icer. Figure 4 shows that the
299 maximum IMC values at 30°F (-1°C) correspond to high inhibitor concentrations, with
300 chloride concentrations in the high range as well.

301 The corrosion impact of the anti-icers on metals was assessed using the
302 electrochemical testing of mild steel exposed to diluted anti-icers and wet-dry cycling.
303 The electrochemical data were ultimately translated to corrosion rate information, in
304 terms of PCR for each diluted anti-icer. The higher the PCR value, the more corrosive the
305 solution is to mild steel. The PCR data were used to establish ANN models, the
306 predictions of which were then used to construct response surfaces. Figure 5 indicates
307 that PCR tends to decrease as the concentration of corrosion inhibitor increases, which
308 confirms the designed role of the inhibitor. The corrosivity of anti-icer to mild steel
309 becomes low (with PCR generally lower than 25) when the inhibitor concentration
310 exceeds 0.06 mL per gram of sodium chloride. Beyond this critical concentration, further
311 increase in the inhibitor concentration shows little benefit in reducing anti-icer
312 corrosivity. It should be cautioned that these findings may change if a different corrosion
313 inhibitor is chosen for anti-icer formulations or if a different metal is considered in the
314 evaluation. Figure 5 also shows that the effect of chloride concentration on PCR is much
315 less obvious.



316
317
318

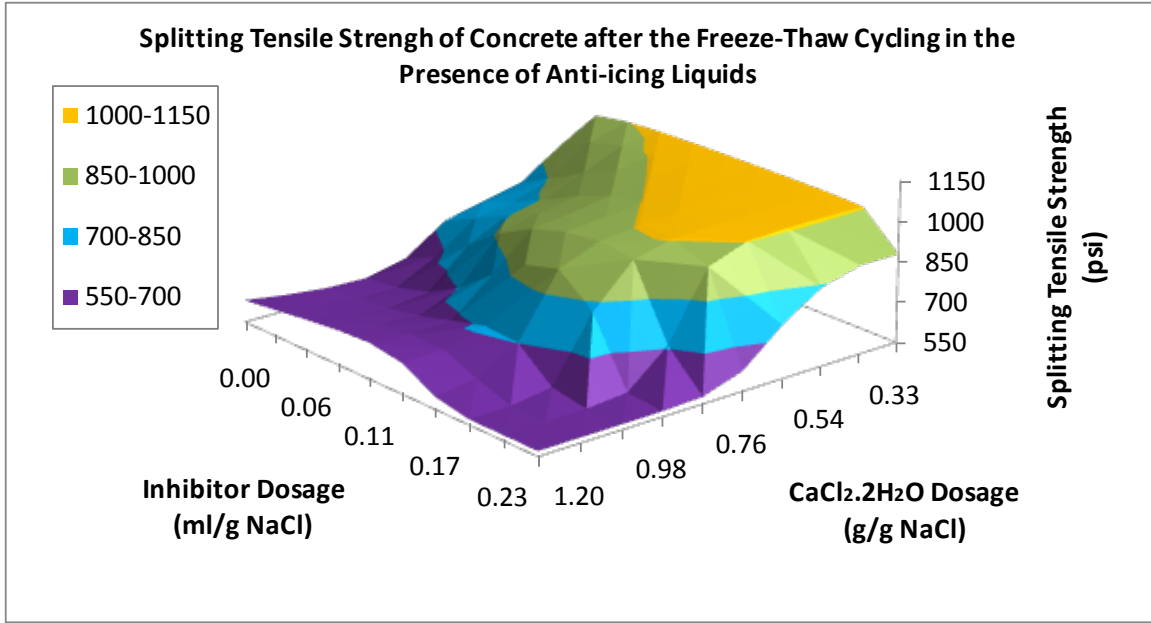
(a)



319
320
321
322
323
324

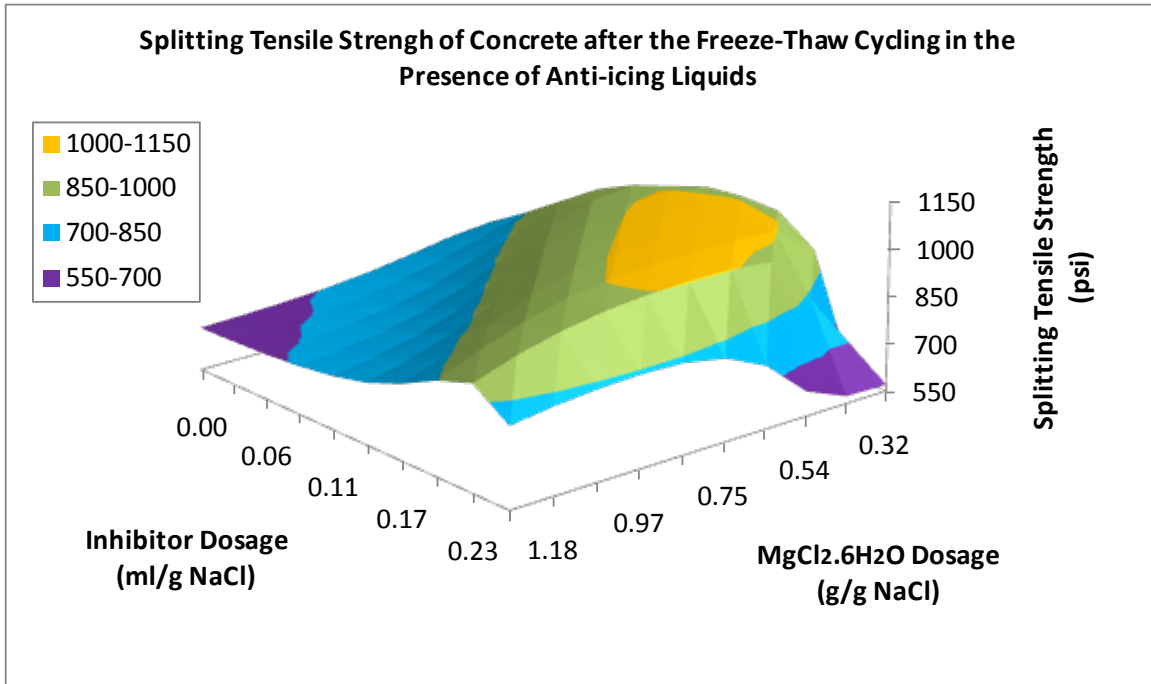
(b)

FIGURE 5 Predicted anti-icer corrosivity as a function of (a) inhibitor and calcium chloride dosages, with $MgCl_2 \cdot 6H_2O/NaCl$ set at 0.65 g/g; (b) inhibitor and magnesium chloride dosages, with $CaCl_2 \cdot 2H_2O/NaCl$ set at 0.65 g/g.



(a)

325
326
327



(b)

328
329
330
331
332
333
334
335

FIGURE 6 Predicted splitting tensile strength of concrete after the freeze-thaw cycling in the presence of anti-icer, as a function of (a) inhibitor and calcium chloride dosages, with MgCl₂·6H₂O/NaCl set at 0.65 g/g; (b) inhibitor and magnesium chloride dosages, with CaCl₂·2H₂O/NaCl set at 0.65 g/g.

336 The impact of the anti-icers on concrete was assessed by exposing PCC
337 specimens to diluted anti-icers and freeze-thaw cycling and subsequently measuring the
338 mass loss of the specimens and testing their *STS*. As shown in Table 1, greater freeze-
339 thaw damage (higher mass loss) is generally associated with reduced *STS*. Note that the
340 indices of freeze-thaw mass loss and *STS* were normalized from actual mass loss (%) and
341 *STS* (psi) by setting the mass loss and *STS* of concrete exposed to water and 3% NaCl as
342 0 and 100 respectively. The freeze-thaw mass loss of concrete exposed to water and 3% NaCl
343 averaged 0.34% and 5.42% respectively, whereas the *STS* of concrete exposed to water and 3%
344 NaCl averaged 1152 psi (7.9 MPa) and 715 psi (4.9 MPa) respectively.

345 The *STS* data were used to establish ANN models, the predictions of which were
346 then used to construct response surfaces. Figure 6 shows that the high *STS* values of
347 concrete, i.e., those greater than 1000 psi (6.9 MPa) correspond to anti-icer formulations
348 with inhibitor and calcium or magnesium chloride by weight of sodium chloride in the
349 range of 0.11-0.23 and 0.43-0.65 respectively. Figure 6(a) indicates that the low *STS*
350 values of concrete (indicative of severe freeze-thaw damage) correspond to high calcium
351 chloride concentrations. Figure 6(b) indicates that the low *STS* values of concrete
352 correspond to either high magnesium chloride concentrations coupled with low inhibitor
353 concentrations, or low magnesium chloride concentrations coupled with high inhibitor
354 concentrations. It should be cautioned that these findings may change if a different
355 corrosion inhibitor is chosen for anti-icer formulations or if a different concrete mix (e.g.,
356 with air entrainment) is considered in the evaluation.

357 The impact of the anti-icers on asphalt was assessed by exposing asphalt binder to
358 anti-icers and thermal and pressure aging and subsequently testing the binder beams with
359 BBR. The BBR test provides values for creep stiffness (higher *S* values correspond to
360 higher thermal stresses so a maximum limit of 300 MPa was specified) and *m*-value
361 (lower *m* values indicate a lesser ability to relax so a minimum limit of 0.30 was
362 specified). We tested a few anti-icer formulations shown in Table 1 (Mix Nos. 5, 7, 8,
363 and 16) that feature the highest and lowest chloride or corrosion inhibitor concentrations
364 in addition to two controls (1: standard practice and 2: exposure to water). The
365 experimental results indicated little effect of anti-icer design on the performance of
366 asphalt binder. In all exposures tested, the *m*-value and stiffness met specifications (fell in
367 0.315-0.333 and 185-207 MPa respectively). As such, the anti-icer impact on asphalt was
368 excluded from further analysis, such as the calculations of composite indices or the
369 modeling process. Acetate-based anti-icers have demonstrated negative effects on asphalt
370 performance, primarily through binder emulsification [5]. If the techniques described in
371 this paper are used to evaluate non-chloride anti-icers, their impacts to asphalt should be
372 investigated for possible inclusion in the comprehensive assessment.

373 Finally, in this study, we assumed the differences in the environmental impacts of
374 the anti-icers and their persistence on the road surface statistically insignificant and thus
375 excluded these target attributes from further analysis. It is desirable to include the
376 environmental impacts of anti-icers into the comprehensive evaluation, especially when
377 chlorides are compared against acetates, formates, or other alternatives and when
378 quantitative or semi-quantitative data of different anti-icers on water quality, air quality,
379 soil, vegetation, wildlife, etc. become available.

380
381

382 **Multi-criteria Decision-making Framework for Anti-icer Formulation**

383 This section will demonstrate a holistic perspective in the design and selection of anti-
 384 icer liquids, by integrating user priorities with the laboratory testing data and cost data. A
 385 recent practitioner survey identified some key desirable attributes of anti-icers, e.g., low
 386 cost per lane mile, low effective temperature, high ice-melting capacity, ease of
 387 application, and overall safety benefits for winter roads. Major concerns regarding anti-
 388 icers included: corrosion to metals, damage to concrete and asphalt pavements, and
 389 reduced water quality [20]. To enable data-driven, multi-criteria decision making, we
 390 present herein four user priority scenarios and describe how in each scenario the anti-icer
 391 formulation could be optimized with the use of a composite index. This type of “*what-if*”
 392 analysis demonstrates how agencies may make more informed, defensible decisions in
 393 selecting, purchasing, or formulating liquids for snow and ice control.

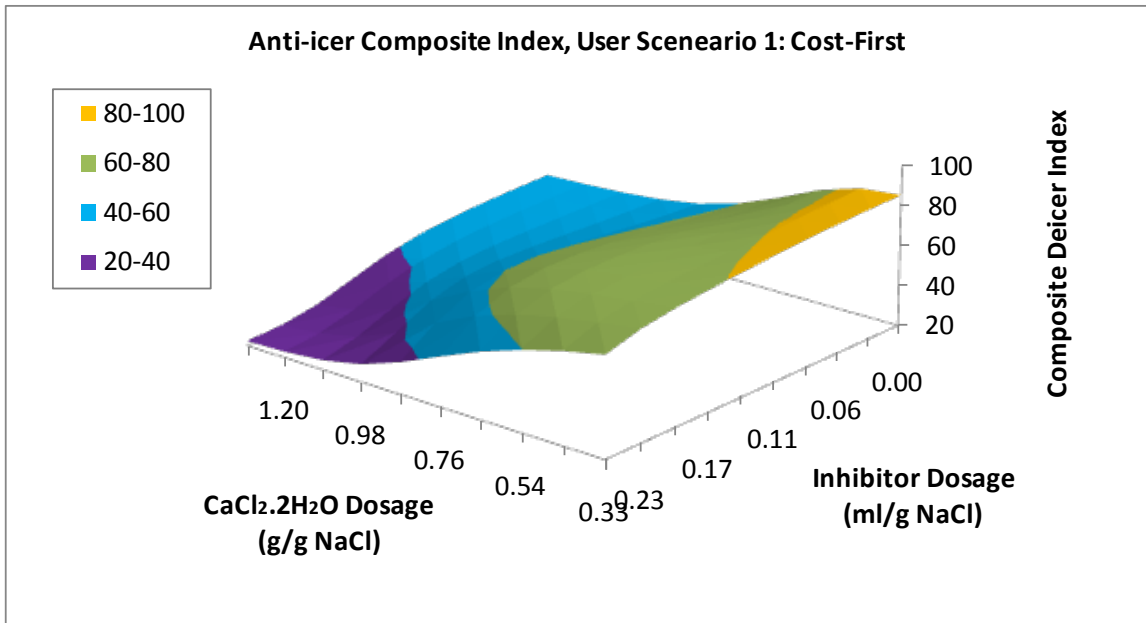
394
 395 **TABLE 3 Decision weights for four possible scenarios**

Scenario	Cost	Characteristic Temperature	Ice Melting Capacity	Corrosion to Metals	Effect on Concrete
1: Cost-first	10	1	1	1	1
2: Effects-first	1	1	1	10	10
3: Performance-first	1	10	10	1	1
4: Balanced-approach	7.0	7.5	7.8	7.9	8.6

397
 398 As shown in Table 3, the four different scenarios to consider are: *cost-first*,
 399 *effects-first*, *performance-first* and a *balanced approach*, each of which places a different
 400 set of decision weights on various target attributes, with 1 being least important and 10
 401 being most important. The decision weights were then normalized so that their sum
 402 across all target attributes becomes 100%. For each anti-icer in Table 1, the values of
 403 each target attribute were first normalized between 0 and 100, with 0 being the worst
 404 performance or most severe impact and 100 being the best performance or least impact.
 405 For the given scenario, the composite index for each anti-icer was calculated by
 406 multiplying the normalized decision weight with the corresponding value of the specific
 407 target attribute before addition across attributes. The *composite index* data were used to
 408 establish ANN models, the predictions of which were then used to construct response
 409 surfaces as shown in Figure 7, which highlights the change of optimal anti-icer
 410 formulation (indicated by high index values) with the user priorities. For instance, the
 411 optimal anti-icer in the *cost-first* scenario would feature low inhibitor concentration,
 412 whereas that in the *effects-first* scenario would feature relatively high inhibitor
 413 concentration, as illustrated by Figures 7(a) and 7(b). In the other two scenarios
 414 illustrated by Figures 7(c) and 7(d), the optimal inhibitor and chloride concentrations fall
 415 in different ranges, relative to the former two scenarios.

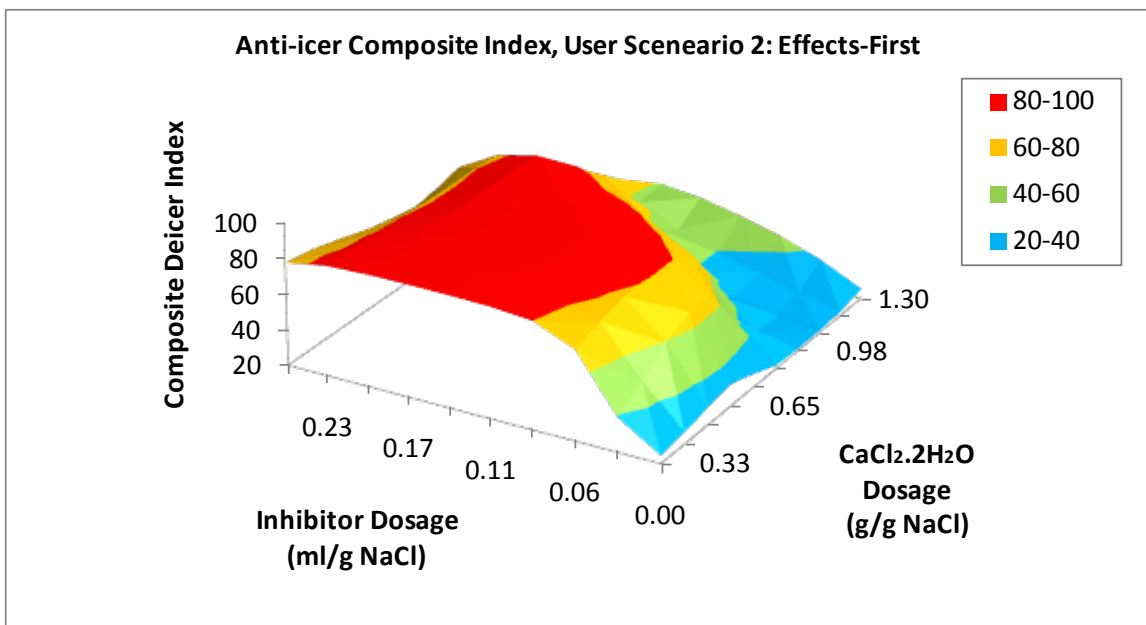
416 Note that the multi-criteria decision-making approach demonstrated herein has its
 417 own caveats and the conclusions derived from the laboratory testing should be used with
 418 caution. For instance, the laboratory testing data may not be good predictors of field

419 performance or impacts, which tend to be site-specific and change as a function of many
420 variables beyond those simulated in the laboratory setting. Existing laboratory tests may
421 not be comprehensive enough to examine all aspects of anti-icers. For instance, the
422 persistence of the chemicals on the road surface is an important aspect to consider when
423 transportation agencies purchase or formulate their anti-icing liquids. Currently there are
424 significant data gaps when it comes to the quantification of environmental impacts of
425 anti-icers (e.g., toxicity to aquatic species) and their longevity on the road surface. These
426 present challenges and knowledge gaps to be addressed by future research.
427



428
429
430

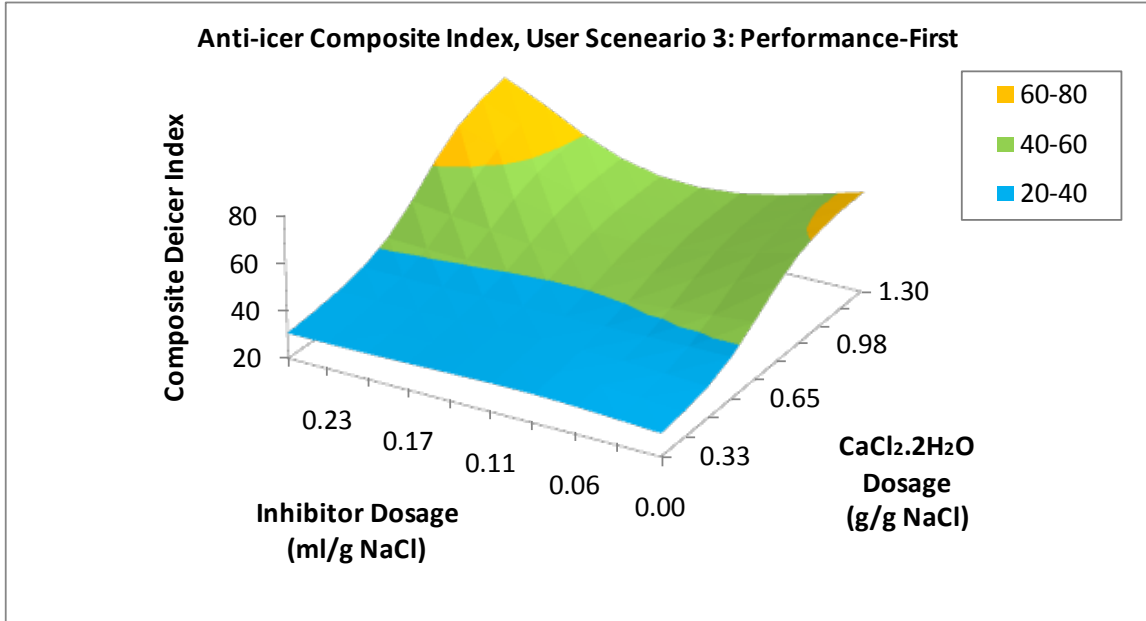
(a)



431
432

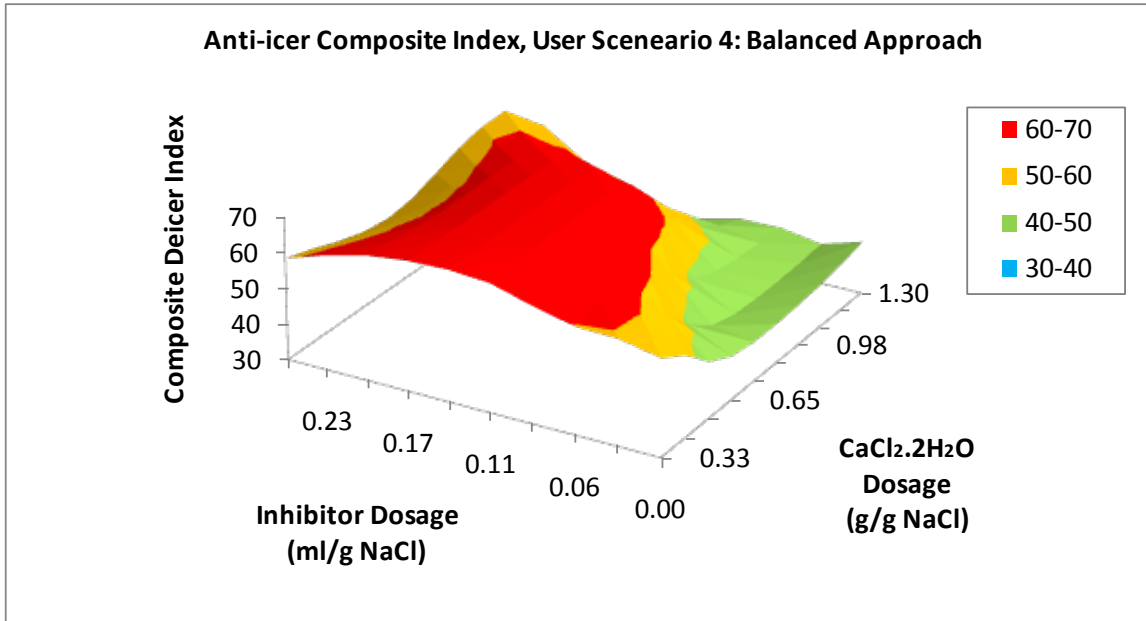
(b)

433
434
435
436
437



438
439
440

(c)



441
442
443

(d)

FIGURE 7 Predicted anti-icer composite index for different user priority scenarios: (a) *cost-first*, (b) *effects-first*, (c) *performance-first*, and (d) *balanced-approach*, as a function of inhibitor and calcium chloride dosages, with $\text{MgCl}_2 \cdot 6\text{H}_2\text{O}/\text{NaCl}$ set at 0.65 g/g.

444
445
446
447

448 **CONCLUSIONS**

449 This work demonstrates a systematic approach to data-driven, multi-criteria decision-
450 making, by conducting a set of laboratory tests to assess twenty blended chloride-based
451 anti-icing formulations. The laboratory data were then used to establish predictive models
452 correlating the multiple design parameters with the anti-icer performance and impacts or
453 with an *anti-icer composite index*. We used artificial neural networks for modeling and
454 examined anti-icer performance (characteristic temperature and ice-melting capacity at
455 30°F and 15°F respectively) and impacts (splitting tensile strength of concrete after ten
456 freeze-thaw cycles and corrosivity to mild steel) as a function of the formulation design.
457 The *anti-icer composite index* was calculated for four different user priority scenarios,
458 each of which placed a different set of decision weights on various target attributes.
459 Response surfaces were then constructed to illustrate such predicted correlations and to
460 guide the direction for formulation improvements. This work also adds to the knowledge
461 base relevant to the performance and impacts of chloride blends.

462

463 **ACKNOWLEDGEMENTS**

464

465 This project was funded by the Research & Innovative Technology Administration
466 (RITA) at the U.S. Department of Transportation, through the University Transportation
467 Center grant to WTI. We thank Bob Evans and Amanda Doornbos of the Montana
468 Department of Transportation for conducting the asphalt tests. We would also like to
469 extend our sincere appreciation to the following colleagues at WTI, Keith Fortune, Levi
470 Ewan, and Marijean Peterson for their assistance with the laboratory testing.

471

472 **REFERENCES**

473

474 [1] Parker, D. *Alternative Snow and Ice Control Methods: Field Evaluation*. Publication
475 FHWA-OR-RD-98-03, Federal Highway Administration, U.S. Department of
476 Transportation, 1997

477 [2] Fischel, M. *Evaluation of Selected Deicers Based on a Review of the Literature*.
478 Publication CDOT-DTD-R-2001-15, Colorado Department of Transportation,
479 2001

480 [3] Staples, J.M., L. Gamradt, O. Stein, and X. Shi. *Recommendations for Winter*
481 *Traction Materials Management on Roadways Adjacent to Bodies of Water*.
482 Publication FHWA/MT-04-008/8117-19, Montana Department of
483 Transportation., 2004.

484 [4] Shi, X., L. Fay, Z. Yang, T.A. Nguyen, and Y. Liu. Corrosion of Deicers to Metals in
485 Transportation Infrastructure: Introduction and Recent Developments. *Corrosion*
486 *Reviews*, Vol. 27, No. 1-2, 2009, pp. 23–52.

487 [5] Shi, X., M. Akin, T. Pan, L. Fay, Y. Liu, and Z. Yang. Deicer Impacts on Pavement
488 Materials: Introduction and Recent Developments. *The Open Civil Engineering*
489 *Journal*, Vol. 3, 2009, pp. 16-27.

490 [6] Fay, L., and X. Shi. Environmental Impacts of Snow and Ice Control Materials: State
491 of the Knowledge. *Journal of Environmental Management*, submitted in 2010.

- 492 [7] O’Keefe, K., and X. Shi. (2005). *Synthesis of Information on Anti-icing and Pre-*
493 *wetting for Winter Highway Maintenance Practices in North America*. Final
494 Report. Pacific Northwest Snowfighters Association and Washington State
495 Department of Transportation, 2005.
- 496 [8] Blackburn R.R., K.M. Bauer, D.E. Amsler, S.E. Boselly, and A.D. McElroy. *Snow*
497 *and Ice Control: Guidelines for Materials and Methods*. Publication NCHRP
498 Report 526. National Cooperative Highway Research Program of the National
499 Academies, Washington, D.C., 2004.
- 500 [9] Conger, S.M. *Winter Highway Maintenance: A Synthesis of Highway Practice*.
501 Publication NCHRP Synthesis 344. National Cooperative Highway Research
502 Program of the National Academies, Washington D.C., 2005.
- 503 [10] Ketcham, S.A., L.D. Minsk, R.R. Blackburn, and E.J. Fleege. *Manual of Practice for*
504 *an Effective Anti-Icing Program: A Guide for Highway Winter Maintenance*
505 *Personnel*. Publication FHWA-RD-9-202. Federal Highway Administration, U.S.
506 Department of Transportation, 1996.
- 507 [11] Warrington, P.D. *Roadsalt and Winter Maintenance for British Columbia*
508 *Municipalities: Best Management Practices to Protect Water Quality*.
509 Publication. Environmental Protection Agency, 1998.
- 510 [12] Perchanok, M.S., D.G. Manning and J.J. Armstrong. *Highway De-Icers: Standards,*
511 *Practices, and Research in the Province of Ontario*. Publication Mat-91-13.
512 Ministry of Transportation of Ontario, 1991.
- 513 [13] Fay, L., K. Volkening, C. Gallaway, and X. Shi. Performance and Impacts of
514 Current Deicing and Anti-icing Products: User Perspective versus Experimental
515 Data. In *TRB 87th Annual Meeting Compendium of Papers DVD*, Transportation
516 Research Board of the National Academies, Washington D.C., 2008.
- 517 [14] Hong Kong Baptist University Department of Mathematics. Uniform Design
518 Website. Undated. <http://www.math.hkbu.edu.hk/UniformDesign/>. Accessed
519 November 27, 2008.
- 520 [15] Akin, M., and X. Shi. *Development of Standardized Test Procedures for Evaluating*
521 *Deicing Chemicals*. Publication. Clear Roads Program and Wisconsin Department
522 of Transportation, 2010.
- 523 [16] Shi, X., and S. Song. Evaluating the Corrosivity of Chemical Deicers: An
524 Electrochemical Technique. Presented at the 16th International Corrosion
525 Congress, Beijing, China, 2005.
- 526 [17] Shi, X., P. Schillings, and D. Boyd. Applying Artificial Neural Networks and Virtual
527 Experimental Design to Quality Improvement of Two Industrial Processes.
528 *International Journal of Production Research*, Vol. 42, No. 1, 2004, pp. 101–108.
- 529 [18] Strong, C., and X. Shi. Benefit-Cost Analysis of Weather Information for Winter
530 Maintenance: A Case Study. *Transportation Research Record*, Vol. 2055, 2008,
531 pp. 119-127.
- 532 [19] Shi, X., Y. Liu, M. Mooney, M. Berry, B. Hubbard, and T.A. Nguyen. Laboratory
533 Investigation and Neural Networks Modeling of Deicer Ingress into Portland

- 534 Cement Concrete and Its Corrosion Implications. *Corrosion Reviews*, Vol. 28,
535 No.3-4, 2010, in press.
- 536 [20] Shi, X., L. Fay, C. Gallaway, K. Volkening, M. Peterson, T. Pan, A. Creighton, C.
537 Lawlor, S. Mumma, Y. Liu, and T.A. Nguyen. *Evaluation of Alternative Anti-*
538 *Icing and Deicing Compounds Using Sodium Chloride and Magnesium Chloride*
539 *as Baseline Deicers—Phase I*. Publication CDOT-2009-1. Colorado Department
540 of Transportation, 2009.